**Supplemental Information includes:**

- **Extended experimental procedures**
- **Supplemental references**
- **Figure legends for figures S1-S6**
- **Table S1**
- **Supplementary figures S1-S6**

**Extended experimental procedures**

**Animals.** 4 month old mice were fed a standard AIN-93G diet (SD; carbohydrate:protein:fat ratio of 64:19:17 percent of kcal) *ad libitum* or at 40% CR, a SD supplemented with 100 mg/$kg_{chow}$ resveratrol *ad libitum*, or a high fat diet *ad libitum* consisting of AIN-93G with 60% of calories from fat, primarily hydrogenated coconut oil (HFD; carbohydrate:protein:fat ratio of 16:23:61). Diets were purchased from Dyets Inc (DSM Nutritional Products North America, Parsippany, NJ). Resveratrol was provided by DSM Nutritional Products (Parsippany, NJ). WT and $Csb^{m/m}$ are on a C57Bl6 background. All measurements were done at 1 year of age. Unless otherwise stated, blood samples were collected after 6 hours of fasting at approximately 6 hours into the light cycle. Body weight and food intake were monitored every other week. Animal rooms were maintained at ~20°C and a 12-hour light/dark cycle. All animal protocols were approved by the Animal Care and Use Committee (352-LEG-2012) of the National Institute on Aging.

**Metabolic assessment.** Metabolic rate of the mice was assessed by indirect calorimetry in open-circuit oxymax chambers using the Comprehensive Lab Animal Monitoring System (CLAMS; Columbus Instruments, Columbus, OH, USA). Mice were single housed and maintained at ~24°C under a 12:12-h light-dark cycle (light period 0600–1800). Water and food were available *ad libitum* except for the CR mice. All mice were acclimatized to monitoring cages for 3-6 h after which twice-hourly, automated recordings of gas exchange were taken over the next 60 h. The concentrations of $O_2$ and $CO_2$ were monitored at the inlet and outlet of the sealed chambers to calculate respiration. The sensors were calibrated against a standard gas mix containing defined quantities of $O_2$, $CO_2$, and $N_2$. Constant airflow (0.6 L/min) was drawn through the chamber and monitored by a mass-sensitive flow meter. Each chamber was measured for 30 s at 30-min intervals. Movement (both horizontal and vertical) was monitored by beams 0.5 in apart on horizontal and vertical planes providing a high-resolution grid

covering the X, Y and Z planes. Beam breaks representing mouse movement were recorded in 30-s epochs. Body composition was measured before and after each trial. Food intake was monitored during the course of the experiment. The respiratory exchange ratio (RER) is simply the ratio between the carbon dioxide production and the oxygen consumption. For PJ34 injection experiments mice were acclimatized to monitoring cages for three days where daily saline injections were given. Body composition was measured using nuclear magnetic resonance spectroscopy before and after starting the experiment Food intake was monitored during the course of the experiment. The respiratory exchange ratio (RER) is simply the ratio between the carbon dioxide production and the oxygen consumption.

**PJ34 and nicotinamide riboside *in vivo* experiment**. 4 or 16 months old $Csb^{m/m}$ or WT male mice maintained on house chow (Harlan Teklad, Madison WI) for the course of the experiment. Five days prior to the experiment mice were handled and restrained daily to become accustomed to handling. At the commencement of the experiment, body composition was measured. Mice were placed into cages in the CLAMS system. Mouse cages were changed every three days. For the initial three days mice were given daily saline injections i.p. at 1100 hours and metabolism was measured as described above. On days 4-10 mice received PJ34 at a dose of 25 mg/kg i.p. (Tocris Bioscience, Bristol, UK) at 1100 hours and metabolism was measured as described above prior to the start of PJ34 treatment and immediately after body composition was measured. For nicotinamide treatments 4 month or 18 month old WT and $Csb^{m/m}$ mice were given daily injections of NR (500 mg/kg/d, ip) or saline for one week after which the mice were sacrificed and the cerebellum was removed for further experiments.

**Body Composition.** Measurements of lean body mass, fat and fluid mass in live mice were acquired by nuclear magnetic resonance (NMR) spectroscopy using the Minispec LF90 (Bruker Optics, Billerica, MA).

**Oral Glucose Tolerance Test (OGTT).** Following a three hour fast, mice received an oral gavage of 30% glucose solution (Sigma Aldrich, St Louis, MO) at a dose of 2g/kg body weight. Blood glucose was measured using an Ascensia Elite glucose meter at 0, 15, 30, 60 and 120 minutes following gavage.

**Serum Chemistry.** Glucose was measured in whole blood using the Ascensia Elite glucose meter (Bayer, Mishawaka, IN). Insulin was measured using an enzyme-linked immunosorbent assay (Crystal Chem, Downers Grove, IL) according to the manufacturer's instructions. Lactate was measured in serum using a Lactate Pro Test Meter according to the manufacturer's instructions (Kyoto, Japan).

**Histology and EM**. Animals were transcardially perfused via with PBS followed by 2.5% glutaraldehyde and 3% paraformaldehyde in PBS. Liver tissue for electron microscopy was transferred to 0.1M sodium cacodylate buffer (Electron Microscopy Sciences, Hatfield PA) for 24 hours at 4C. For transmission electron microscopy, samples were osmicated and embedded in Spurs resin. Ultra-thin (70-90nm) sections were taken from each block and twenty random fields were chosen from each liver and photographed for ultrastructural measurement using a Phillips CM10 Transmission Electron Microscope (magnification 1950x). Mitochondrial area was determined using image J (http://rsb.info.nih.gov/ij/). For scanning electron microscopy samples were osmicated, dehydrated, mounted and coated with platinum and liver sinusoidal endothelial porosity (percentage of the endothelial surface area occupied by fenestrations) was manually calculated on 10 sinusoids per liver using image J. The cerebellum was cut

into small specimens (typically 0.5 mm×0.5 mm×1 mm). The specimens were cryoprotected in glycerol and freeze substituted with Lowicryl HM20 according to an electron microscopic immunogold protocol (Bergersen et al., 2008). Ultrathin sections were cut (90 nm) using a diamond knife and dried at room temperature. The dried sections were counterstained with 1% uranyl acetate and 0.3% lead citrate. Electron micrographs were taken with a FEI Tecnai 12 electron microscope at primary magnifications of ×26500 and saved as tif files. Postsynaptic densities (PSDs) were identified in dendritic spines by their electron dense appearance, forming asymmetric synapses with nerve terminals. The length of the PSD was measured using ImageJ (http://imagej.nih.gov/ij/) and the "DistToPath" plugin (http://www.neuro.ki.se/broman/maxl/software.html). Histology of the liver and inner ear was performed by Histoserv (Histoserv, MD, USA) on the transcardially fixated tissue by staining with Masson's trichrome and hematoxylin and eosin respectively.

**Microarray.** Gene expression of WT and $Csb^{m/m}$ cerebellum was performed. Raw hybridization intensity data were log-transformed and normalized to yield z-scores. The z-ratio was calculated as the difference between the observed gene z-scores for the experimental and the control comparisons, and dividing by the standard deviation associated with the distribution of these differences. Z-ratio values =+2.0 or =-2.0 were chosen as cut-off values, defining increased and decreased expression, respectively. A complete set of 522 cellular pathways was obtained from the Molecular Signatures Database (MSigDB, Broad Institute, Massachusetts Institute of Technology, MA, USA). The complete set was tested for Geneset enrichment using Parametric analysis of Gene set enrichment (PAGE). For each pathway z-score, a p-value was computed using JMP 6.0 software to test for the significance of the z-score obtained. Principal component analysis was done using JMP 6.0. These tools were part of DIANE 1.0 (see http://www.grc.nia.nih.gov/branches/rrb/dna/diane_software.pdf for information).

**Metabolomics.** Metabolomic measurements were acquired by the West Coast Metabolomics Center. Briefly, mouse cerebellum tissue 20 mg FW was extracted using 1 mL of degassed acetonitrile:isopropanol:water (3:3:2; v/v/v) at -20°C, evaporated to dryness, and membrane lipids and triglycerides were removed in a clean-up using acetonitrile/water (1:1). Internal retention standards were added and samples were derivatized by 10 µL methoxyamine hydrochloride in pyridine (40 mg/ml) followed by 90 µl MSTFA (1 mL bottles, Sigma-Aldrich) for trimethylsilylation of acidic protons. Metabolomic analysis was conducted by injecting 0.5 µL of sample using a Gerstel MPS2 automatic liner exhange system (Mülheim, Germany) with cold injection system, separation on an Agilent 6890 gas chromatograph (Santa Clara, CA) equipped with a 30 m long, 0.25 mm i.d. Rtx5Sil-MS column, and mass spectra acquisition by a Leco Pegasus IV time of flight mass spectrometer (St. Joseph, MI) at a mass range of m/z 85–500 at 17 spectra s-1 and 1850V detector voltage, aquired with 280°C transfer line temperature, electron ionization at -70eV and an ion source temperature of 250°C. Result files were processed by BinBase database (http://fiehnlab.ucdavis.edu/projects/binbase_setupx), by matching retention index and mass spectra against the Fiehn mass spectral library of 1,200 compounds and the NIST05 commercial library. Final data were normalized to the average sum intensities for all known metabolites.

**Open field**. A mouse was placed in the center of a Plexiglas square measuring 23 inches X 23 inches. The open field was evenly illuminated and exploratory behavior was measured for 300 seconds using AnyMaze software (Wood Dale, IL). The apparatus was cleaned with 70% ethanol before testing the next mouse.

**Treadmill**. Mice were required to exercise on the treadmill until exhaustion. The treadmill was horizontal (0° incline) and mice ran in groups of 6. Subjects were habituated at a constant speed of 4 m/min for 5 minutes on day 1. The following day each mouse was given a trial starting at 7 m/min for 0-3 minutes, 12 m/min for 3-7 minutes, 15 m/min for 7-25 minutes, and 19 m/min for 25 minutes.

**Hearing test.** Mice were placed in a clear, plastic, rectangular box (23 inches x 23 inches) for a total of 300 seconds. Video and movement tracking were captured using ANY-Maze software (Stoelting Co. Wood Dale, IL). Two speakers, connected to a laptop, were placed at one end of the box on the same level as the top of the box. At 295 seconds, a previously recorded clap (108 db) was played on the speakers in order to test the capability of the mice to display a proper startle response when hearing a loud noise. Mice were subsequently scored for no response, possible response and definite response based on the video recording.

**Cell culture.** SV40-transformed CS1AN cells stably transfected with either CSB (WT CSB) or empty vector were cultured in DMEM supplemented with 10% FBS, 1% pen-strep, and 400 μg/ml geneticin and grown in 20% O2/5% CO2 at 37°C. PARP1 knockout HeLa cells were a kind gift of A. Mangerich, A. Bürkle, E. and Ferrando-May. Treatments done: resveratrol 100 μM for 48 hours; Srt1720 3 μM for 48 hours; NU1025 100 μM for 48 hours; PJ34 10 μM for 48 hours; 3AB 1 mM for 48 hours; β-OH-butyrate 10 mM for 48 hours; A-769662 10 μM for 48 hours; AICAR 1 mM for 48 hours; Dorsomorphin 5 μM for 48 hours; 3%$O_2$ treatment 72 hours; LW6 2.5/5 μM for 48 hours; siRNAs for 72 hours; 0.5 mM Oleic acid for 72 hours; 5 mM glucose for 72 hours; 100 μM EX-527 for 24 hours; 5/10/20 μM L002 for 24 hours; 50 μM MB-3 for 24 hours; 10 μM NU9056 for 24 hours; 5 μM C646 for 24 hours; 10 μM MG-132 for 5 hours.

**Cellular oxygen consumption**. Oxygen consumption and extracellular acidification rate measurements were performed using the Seahorse XF-24 instrument (Seahorse Biosciences, North Billerica, MA, USA). Cells were seeded into a Seahorse tissue culture plate. 24 h later media was changed to unbuffered XF assay media, pH 7.4 (Seahorse Biosciences, North Billerica, MA, USA) supplemented with 25 mM glucose (Sigma-Aldrich, St. Louis, MO, USA) and 1 mM sodium-pyruvate and 1 mM glutamax (Invitrogen, Carlsbad, CA, USA). Cells were incubated for 1 h at 37 °C at ambient $O_2$ and $CO_2$ levels. Respiration was measured in 4 blocks of 3 times 3 minutes. The first block measured the basal respiration rate. Next oligomycin (EMD chemicals, Gibbstown, NJ, USA) was added and the second block was measured. Then carbonyl cyanide 4-(trifluoromethoxy) phenylhydrazone (FCCP) (Sigma-Aldrich, St. Louis, MO, USA) was added and the third block was measured. Finally antimycin A (Sigma-Aldrich, St. Louis, MO, USA) was added and the last measurements were performed. Immediately after finishing the measurements cells were trypsinized and counted using a coulter counter (Beckman Coulter Inc., Brea, CA, USA). Lactate equilibrium was performed with XF-assay media supplemented with 25 mM glucose. First injection was 100 mM 2-deoxyglucose and subsequent injections were lactate (pH 7.4) as indicated.

**Mitochondrial isolation and oxygen consumption.** Tissues were homogenized in MAS-buffer (mannitol, sucrose, hepes) using a glass-teflon homogenizer and nuclei/debris was precipitated by a 1.000 g centrifugation for 10 minutes, 4°C. Supernatants were transferred to new tubes and mitochondria were precipitated by a 6.000 g centrifugation for 7 minutes, 4°C. The mitochondria were washed in MAS buffer and precipitated by a 6.000 g centrifugation for 7 minutes, 4°C. Mitochondria were resuspended in 500 µL MAS and 20 µL was injected into a pre-calibrated chamber in the Oroboros oxygraph (Oroboros, Innsbruck, Austria) containing 2 mL MAS supplemented with 5 mM succinate, 5 mM

pyruvate and 2 mM malate. State-4 respiration was measured and 3 mM ADP was injected and state-3 respiration was measured. The remaining mitochondrial suspension was flash frozen in liquid nitrogen and used for protein and citrate synthase measurements. For membrane potential and ROS production mitochondria were incubated for 15 minutes at 37°C in MAS supplemented with 5 mM succinate, 5 mM pyruvate and 2 mM malate, and 40 nM TMRM or 3 μM dihydroethidium.

**NAD and ketone measurements**. The NAD/NADH ratio was measured using a kit and following the provided protocol (Abcam, Cambridge, UK). For mass spectrometry $10^7$ cells were suspended in 50 μl of deionized water, to which 250 μl of acetonitrile was added. The suspension was vortexed for 1 min, followed by centrifugation at 16,000 g at 4$^{o}$C for 5 min. The supernatant was collected and analyzed by mass spectrometry. The separations of the compounds were accomplished using a Zorbax XDB-C18 analytical column (50 x 4.6 mm i.d., 1.8 μm particles) purchased from Agilent (Palo Alto, CA, USA) following a previously described method with slight modification [reference below]. In brief, a linear gradient was run as follows: 0-5 min 10%B; 5-14 min 100%B; 14-15 min 100%B; 15-16 min 10%B; 16-20 min 10%B at a flow rate of 0.4 ml/min. The mobile phase consisted of water containing 0.05% trifluoroacetic acid (TFA) for component A and acetonitrile containing 0.02% TFA for component B. The total run time was 20 min per sample. Injection volume per sample was 50 μl. MS analysis was performed using an Agilent Technologies 1100 LC/MSD (Palo Alto, CA, USA) equipped with a G1322A degasser, G1312A binary pump, G1367A autosampler, G1316A column thermostat, G1315A diode array detector and G1946D mass spectrometer equipped with an electrospray ionization (ESI) interface. The analytes were monitored in the positive-ion mode for SIM at m/z 123.1 ($[M+H]^+$ of NAM), 335.1 ($[M+H]^+$ of NMN) and 664.1 ($[M+H]^+$ of NAD). Ketone bodies (β-hydroxybutarate) were measured in serum using a kit according to the manufacturer's instructions (Cayman Chemicals, Ann Arbor MI). ß-

hydroxybutyrate (BHB) levels in the brain tissue samples were measured using a previously described and validated LC/MS/MS method (Johansen and Windberg, 2011). In brief, brain tissue was spiked with 50 µL of 1 mM γ-hydroxybutyrate-$d_6$ (GHB-$d_6$). The sample was homogenized with 950 µL methanol. The sample was centrifuged at 14000 rpm for 15 min. The supernatant was analysed using a LC/MS/MS system. The chromatographic experiments were carried out on a Shimadzu Prominence high-performance liquid chromatography system (Shimadzu, Columbia, Maryland), and total analyte concentrations were determined using Zorbax SB C18 column (150 x 2.1 mm, Agilient technologies). An elution gradient, with mobile phases consisting of acidic water (0.1 % formic acid) and acidic methanol (0.1 % formic acid) (0–10 min: 0–10%; 11–16 min: 10–80%) respectively, separated the compounds within 20 min was utilized. The tandem mass spectrometry analysis was performed using a triple quadrupole mass spectrometer model API 4000 system from Applied Biosystems/MDS Sciex equipped with Turbo Ion Spray (Applied Biosystems, Foster City, California). Data were acquired and analyzed using Analyst version 1.4.2 (Applied Biosystems). Positive electrospray ionization data were acquired using multiple reaction monitoring, and quantification was accomplished using area ratios calculated using BHB-$d_6$ as the internal standard, where the concentration of the internal standard was set at 50 µM.

**Acetyl-CoA measurements**. Were performed using a kit and following the provided protocol (Sigma-Aldrich, St. Louis, MO, USA).

**Acid extraction of histones.** Histone were isolated as previously described (Shechter et al., 2007). Cells were preincubated at 2 mM glucose for 48 hours prior to treatments with 10 mM β-OH-butyrate or 10 µM PJ34.

**Western, far-western and slot-blotting**. Poly(ADP-ribose) was synthesized and purified as described previously (Popp et al., 2013). Purified recombinant proteins were either separated via denaturing polyacrylamide gel electrophoresis followed by semi-dry blotting or were directly immobilized on a nitrocellulose membrane using a slotblot manifold and vacuum. Subsequently, membranes with immobilized proteins were incubated with 0.2 µM poly(ADP-ribose) in TBST over night at 4°C, followed by high-stringency washes using 1M NaCl inTBST (3 times for 5 min at RT). Non-covalently bound poly(ADP-ribose) was detected using the anti-poly(ADP-ribose)-specific mAB 10H, anti-mouse HRP-coupled secondary antibody, and chemiluminescence detection.

**Materials.** Antibodies used in the study were purchased from the below companies: PAR (BD Pharmingen, #551813), PARP1 (Cell signaling, #9542), PARG1 (Abnova company, #H00008505-B01P), actin (abcam, #ab6276), Sirt1 (Santa Cruz, #sc-74465), Sirt2 (abcam, #ab51023), Sirt3 (Cell signaling, #5490), Sirt4 (Sigma, #S0948), Sirt5 (Sigma, #HPA022002), Sirt6 (Cell signaling, #12486), Sirt7 (Millipore, #ABE103), Bax (Cell signaling, #2772), Bcl-xL (Cell signaling, #2764), Bcl-2 (Cell signaling, #50E3), p65 (Cell signaling, #6956), ace-p65 (Cell signaling, #3045), p53 (Santa cruz,#SC-71818), ace-p53 (Cell signaling, #2570), UCP2 (Lifespan, #Ab-LS-B3249), Sir2.1 (Novus, #NB100-1923), PDK1 (Novus, #NB100-2383), PDK2 (abcam, #ab68164), PDK3 (Novus, #NBP1-54707), and PDK4 (abcam, #ab38242). A CSB antibody was raised in a rabbit against a peptide containing the c-terminal 1100-1300 amino acids of CSB and subsequent affinity purified against the antigen. siRNA against SIRT1, UCP2, p300, CBP, GCN5, PCAF, HIF-1α and HIF-2α were purchased from Origene.

**Nematode studies.** Bristol N2 (wild type) and csb-1 worms (ok2335) were purchased from the Caenorhabditis Genetics Centre (CGC) at the University of Minnesota, St. Paul, MN. csb-1 worms were outcrossed five times to the N2 prior to use. Lifespan analysis was performed at 25 °C for grown on classical NGM plates, or NGM plates supplemented with 25 mM β-hydroxybutyrate seeded with E. coli OP50 as food source (Fensgard et al., 2010). 25 L4 stage worms (Day 0) were transferred to 2 plates, to give synchronous populations of 50 animals per condition. Animals were scored as dead or alive and transferred every day to fresh plates seeded with E. coli OP50 during the fertile period, and then every day until death. Worms were considered dead when they stopped pharyngeal pumping and were unresponsive to touch. Worms that died because of internal bagging, desiccation due to crawling on the edge of the plates, or gonad extrusion were scored as censored. These animals were included in life-span analyses up to the point of censorship and were weighted by half in mortality calculations. We calculated mean, standard deviation of the mean, and P value using the log-rank test, from pooled population of animals. Figures display Kaplan Meier survival curves of pooled populations utilized for statistical analysis.

**Microscopy**. $5 \times 10^4$ cells were plated in 4 well chamber slides and grown overnight and fixed for 15 minutes in 3.7% paraformaldehyde in PBS. Cells were then washed before being permeabilized in 0.25% triton X-100 for 10 minutes on ice. Subsequently cells were washed in PBS and blocked over-night in PBS containing 5% FBS. Primary antibodies were added at a concentration of 1:100 and incubated for 1 hour at 37˚C. After being washed secondary antibodies were added at 1:1000 and incubated for 1 hour at 37˚C. Cells were then washed 6 times 10 minutes in PBS before being mounted in prolong antifade gold with DAPI (Invitrogen, Carlsbad, CA, USA). Images were acquired at 60 × magnification on a Nikon Eclipse

TE-2000e confocal microscope (Nikon, Tokyo, Japan). Quantification of foci was done using Volocity software (PerkinElmer, Waltham, MA, USA).

**Flow cytometry.** $2 \times 10^5$ cells were seeded in a 6 well culture dish. 24 hours later cells were washed in PBS once and trypsinized. Cells were then resuspended in DMEM without phenol red supplemented with 10% FBS containing 50 nM mitotracker Green FM (Invitrogen, Carlsbad, CA, USA), 20 nM TMRM (Invitrogen, Carlsbad, CA, USA) , 3 μM dihydroethidium (Invitrogen, Carlsbad, CA, USA) or 3 μM mitosox (Invitrogen, Carlsbad, CA, USA). Cells stained with TMRM were incubated for 15 minutes at 37°C while 30 minutes incubations were used for the rest of the stains. Fluorescence was measured by a flow cytometer (C6 Flow Cytometer, Accuri, Michigan, USA).

**Biochemistry and recombinant proteins.** PARP1 was purchased from Trevigen. Recombinant CSB was a gift from Dr. Tinna Stevsner. PARP1 activity was investigated by incubating 30 nM PARP1 with increasing doses of purified CSB in the presence of 10 nM double stranded DNA in the reaction buffer (1 mM $NAD^+$, 10 mM TRIS-HCl pH 8.0, 1 mM $MgCl_2$, 1 mM DTT) for 10 minutes at 37°C. The product was visualized by western blotting. UV-damaged DNA was generated by exposing a 39-mer double stranded DNA oligo to UV radiation for 10 minutes. Electro-mobility shift assay (EMSA) was performed by incubating PARP1 with DNA for 10 minutes at 37C after which increasing doses of CSB was added and further incubation was done for another 20 minutes at 37C. Reactions were performed in 20 mM HEPES-OH pH 8.0, 50 mM KCl, 200 μg/mL BSA, 5 mM DTT, and 5% (v/v) glycerol. Finished reactions were run on a 4% native polyacrylamide gel and visualized by Sybr Gold staining (Invitrogen, Carlsbad, CA, USA) on a ChemiDocTM MP (Bio-Rad, Hercules, CA, USA). BamH1 assay was performed by preincubating a 42-mer oligo containing a single BamH1 restriction site with 250 nM PARP1 for 20 minutes at 37C with or

without $NAD^+$. 125, 250 or 500 nM of CSB and 0.2 U BamH1-HF (New England Biolabs, Ipswich, MA,USA) was subsequently added and the reaction was further incubated 30 minutes at 37C. The reaction was performed in 20 mM HEPES-OH pH 8.0, 50 mM KCl, 4 mM $MgCl_2$, 200 µg/mL BSA, 5 mM DTT, and 5% (v/v) glycerol. The finished reaction was run on a 10% native gel and visualized by Sybr Gold staining (Invitrogen, Carlsbad, CA, USA) on a ChemiDocTM MP (Bio-Rad, Hercules, CA, USA).

**Site-directed mutagenesis for substitutions K292A, K297A, K334A and K337A on CSB in CSB-GFP plasmid.** Multiple substitutions for K292A, K297A, K334A and K337A on CSB in CSB-GFP plasmid was performed using QuikChange II Site-Directed Mutagenesis Kit (Agilent Technologies). The specific nucleotide changes corresponding to K292A and K297A on CSB in the plasmid was completed and then substitution for K334A and K337A was carried out. The two primer sets contain with the relevant nucleotide changes of K292A/K297A (forward primer; 5'-GTAATGCAAGAGCAGCTAGAGCAGCTCCAGCCCCAGTCACG-3', reverse primer; 5'-CTCGACGAGATCGACGAGAACGTAATGTTGGAACGAAGAA-3'), or K334A/K337A (forward primer; 5'-CCCTGGAACTGCAAAGCCCTCGCCTGGAGTGCCTTGATGTGCTTTTTCAAACG-3', reverse primer; 5'-CGTTTGAAAAAGCACATCAAGGCACTCCAGGCGAGGGCTTTGCAGTTCCAGGG-3'), respectively. PCR was carried according to the manufacturer's instruction. After digestion with DpnI (TaKaRa, Shiga, Japan), the DNA mix was transformed into NEB 5-alpha Competent E. coli (High Efficiency) (New England Biolabs) and then selected clones were sequence confirmed by Eurofins Genomics (Huntsville, AL, USA).

**Protein Recruitment and Retention Experiments.** To monitor protein recruitment and retention to laser induced DNA damage, localized microirradiation was performed as previously described in detail (McNeill et al., 2013). In brief, HeLa cells ($2.0 \times 10^5$ cells) were precultured in a 35-mm glass bottom

culture dish with 10 mm diameter microwells (MatTek Corporation, Ashland, MA, USA) for 24 hr. GFP-tagged CSB (CSB-GFP) plasmid was transfected using JetPrime reagent (Polyplus-transfection, Illkirch, France) according to the manufacturer's standard protocol. The transfected cells were incubated for 24 hr before micropoint laser experiment. A 5 × 20 pixel (0.16 µm/pixel) region internal to the nuclei of the cells was targeted using a Plan Fluor ×60/1.25 numerical aperture oil objective. Throughout the experiment, the adhered cells were maintained at 80% humidity, 5% $CO_2$, and 37 °C using a live cell environmental chamber (Slonet Scientific, Segensworth, UK). To determine the effects of PARP inhibition on recruitment of CSB, 10 µM PJ-34 or 1 mM 3AB was added to the media one hour prior to laser microirradiation. The images were recorded using identical gain, exposure, sensitivity, and contrast settings, and analyzed with the Volocity software 6.2 (PerkinElmer, Waltham, MA, USA).

**Statistics**. Two-way ANOVA was used to determine significant difference across genotypes. Two-tailed t-tests were used to compare single groups using Graphpad prism (GraphPad Software, Inc., La Jolla, CA, USA).

Reference List

Bergersen,L.H., Storm-Mathisen,J., and Gundersen,V. (2008). Immunogold quantification of amino acids and proteins in complex subcellular compartments. Nat. Protoc. *3*, 144-152.

Johansen,S.S. and Windberg,C.N. (2011). Simultaneous determination of gamma-Hydroxybutyrate (GHB) and its analogues (GBL, 1.4-BD, GVL) in whole blood and urine by liquid chromatography coupled to tandem mass spectrometry. J. Anal. Toxicol. *35*, 8-14.

McNeill,D.R., Paramasivam,M., Baldwin,J., Huang,J., Vyjayanti,V.N., Seidman,M.M., and Wilson,D.M., III (2013). NEIL1 responds and binds to psoralen-induced DNA interstrand crosslinks. J. Biol. Chem. *288*, 12426-12436.

Popp,O., Veith,S., Fahrer,J., Bohr,V.A., Burkle,A., and Mangerich,A. (2013). Site-specific noncovalent interaction of the biopolymer poly(ADP-ribose) with the Werner syndrome protein regulates protein functions. ACS Chem. Biol. *8*, 179-188.

Shechter,D., Dormann,H.L., Allis,C.D., and Hake,S.B. (2007). Extraction, purification and analysis of histones. Nat. Protoc. *2*, 1445-1457.

**Supplementary figure legends**

**Figure S1, related to figure 1.** (A-C) daily food intake in the mice (n=12-14, mean ± SEM). (D-G) temperature levels in the mice (n=12-14, mean ± SEM). (H) and (I) Ambulatory movement of the mice in the metabolic cages as measured by double line breaks (n=12-14, mean ± SEM). (J) Representative images of transmission electron microscopy of the sinusoidal endothelium (e: endothelium, s: sinusoid, h: hepatocyte).

**Figure S2, related to figure 2.** (A) Venn diagrams of significantly changed genes when comparing HFD treatment to SD and HFD treatment to Resv. (B) Representative electron microscopy micrographs of the cerebellum of the mice (m: mitochondria, pf: Purkinje fibre, a: astrocyte, s: post-synaptic fibre, v: synapse). (C) Synaptic length (n=100-300, mean ± SEM). (D) Rotarod performance (n=11-14, mean ± SEM).

**Figure S3, related to figure 2.** (A) Distance travelled in open field test (n=11-14, mean ± SEM). (B) Speed travelled in the open field test (n=11-14, mean ± SEM). (C) Percent distance spend in the center in the open field test (n=11-14, mean ± SEM). (D) Distance travelled in a forced treadmill exercise (n=7-11, mean ± SEM). (E) Grip strength as measured by the time to fall from a wire of mice hanging by the for-limbs (n=11-14, mean ± SEM). (F) State-4 respiration of isolated mitochondria from the brain (n=5-8, mean ± SEM). (G) Respiratory control ratio (state-3 / state-4) (n=5-8, mean ± SEM). (H) State-3 respiration in isolated whole brain mitochondria after addition of 3 mM ADP using 2 mM malate, 4 mM succinate and 4 mM pyruvate as substrates (n=5-8, mean ± SEM). (I) State-4 respiration in isolated liver mitochondria (n=5-9, mean ± SEM). (J) State-3 respiration in isolated liver mitochondria after addition of 3 mM ADP using 2 mM malate, 4 mM succinate and 4 mM pyruvate as substrates (n=5-9, mean ± SEM). (K) The respiratory coupling ratio of liver mitochondria (n=5-9, mean ± SEM).

**Figure S4, related to figure 2.** (A) Lactate stimulated respiration of WT and CSB cells after inhibition of glycolysis and without other mitochondrial substrates in the assay medium (n=3 separate experiments, mean ± SEM). (B) Representative immunoblot of pyruvate dehydrogenase kinase isoforms in the cerebellum of WT and $Csb^{m/m}$ mice. Each lane is a separate mouse. (C) The lactate pyruvate equilibrium.

**Figure S5, related to figure 5.** (A) Alterations in the FCCP uncoupled respiration relative to basal respiration in WT and CSB cells (n=3-28 separate experiments, mean ± SEM). (B) Representative immunoblot of UCP2 protein levels in CSB and WT cells after transfection with a UCP2 encoding plasmid or knockdown using siRNA.

**Figure S6, related to figure 4 and 6.** (A) Flow cytometry of WT and CSB deficient cells treated with β-OHB and or EX-527 for 48 hours and stained with TMRM (n=6, mean ± SEM). (B) Representative immunoblot of SIRT1 and PAR levels after inhibition with PARP inhibitors. (C) Growth curves of WT and CSB deficient cells treated with increasing concentrations of L002 (n=3, mean ± SD). (D) Flow cytometry of WT and CSB deficient cells treated with MB-3, NU9056 or increasing concentration of L002 for 24 hours and stained with TMRM (n=3-12, mean ± SEM) (E) Growth curve of WT and CSB deficient cells treated with the histone acetyl transferase inhibitors MB-3 and NU9056. (F) Flow cytometry of WT and CSB deficient cells treated with C646 and stained with TMRM or mitosox (n=3, mean ± SEM). (G) Flow cytometry of WT and CSB deficient cells subjected to siRNA knockdown of various proteins and stained with TMRM (n=3, mean ± SEM). (H) Luciferase based SIRT1 promotor activity assay showing luminescence from WT and CSB deficient cells subjected to 24 hours L002 treatment (data normalized to ACTB promotor activity, n=3-6, mean ± SEM). (I) Representative far western of non-covalent CSB-PAR interaction.

| GENE ONTOLOGY TERM | CSB saline vs WT (Z-score) | CSB saline vs WT (P-value) | CSB NR vs WT (Z-score) | CSB NR vs WT (P_value) |
|---|---|---|---|---|
| 8137 NADH DEHYDROGENASE (UBIQUINONE) ACTIVITY | 6.50 | 1.24E-15 | 1.10 | 0.24 |
| 4129 CYTOCHROME C OXIDASE ACTIVITY | 5.44 | 2.52E-06 | 0.85 | 0.53 |
| 3954 NADH DEHYDROGENASE ACTIVITY | 4.65 | 5.62E-14 | 0.67 | 0.34 |
| 5743 MITOCHONDRIAL INNER MEMBRANE | 4.23 | 6.77E-04 | -1.26 | 0.33 |
| 5739 MITOCHONDRION | 3.98 | 2.30E-04 | 0.59 | 0.59 |
| 15986 ATP SYNTHESIS COUPLED PROTON TRANSPORT | 3.28 | 1.51E-05 | 1.30 | 0.22 |
| 5746 MITOCHONDRIAL RESPIRATORY CHAIN | 3.18 | 3.20E-03 | 0.14 | 0.90 |
| 46961 HYDROGEN ION TRANSPORTING ATPASE ACTIVIT | 3.14 | 1.78E-04 | 1.82 | 0.07 |
| 16469 PROTON TRANSPORTING TWO SECTOR ATPASE CO | 3.12 | 2.73E-05 | 1.79 | 0.08 |
| 46933 PROTON-TRANSPORTING ATP SYNTHASE ACTIVITY, ROTATIONAL MECHANISM | 3.10 | 2.65E-04 | 1.71 | 0.09 |
| 302 RESPONSE TO REACTIVE OXYGEN SPECIES | 2.74 | 1.49E-02 | 2.06 | 0.22 |
| 6122 MITOCHONDRIAL ELECTRON TRANSPORT, UBIQUINOL TO CYTOCHROME C | 2.71 | 4.16E-03 | 0.62 | 0.64 |
| 45261 PROTON TRANSPORTING ATP SYNTHASE COMPLEX | 2.67 | 1.10E-07 | 1.06 | 0.43 |
| 5751 MITOCHONDRIAL RESPIRATORY CHAIN COMPLEX | 2.64 | 6.50E-03 | 0.44 | 0.52 |
| 45263 PROTON TRANSPORTING ATP SYNTHASE COMPLEX | 2.57 | 1.59E-02 | 1.50 | 0.07 |
| 19825 OXYGEN BINDING | 2.51 | 3.00E-03 | 0.39 | 0.80 |
| 6950 RESPONSE TO STRESS | 2.50 | 4.60E-02 | 0.85 | 0.54 |
| 5747 MITOCHONDRIAL RESPIRATORY CHAIN COMPLEX | 2.48 | 1.08E-03 | 0.64 | 0.56 |
| 6626 PROTEIN TARGETING TO MITOCHONDRION | 2.32 | 2.04E-02 | 0.87 | 0.22 |
| 5753 MITOCHONDRIAL PROTON-TRANSPORTING ATP SYNTHASE COMPLEX | 2.32 | 3.03E-03 | -0.40 | 0.69 |
| 45454 CELL REDOX HOMEOSTASIS | 2.00 | 4.29E-02 | 0.13 | 0.90 |
| 6120 MITOCHONDRIAL ELECTRON TRANSPORT, NADH TO UBIQUINONE | 1.99 | 4.76E-03 | 0.68 | 0.35 |
| 42542 RESPONSE TO HYDROGEN PEROXIDE | 1.83 | 3.27E-02 | 0.52 | 0.53 |
| 16651 OXIDOREDUCTASE ACTIVITY  ACTING ON NADH | 1.80 | 4.54E-03 | 0.51 | 0.60 |
| 7568 AGING | 1.52 | 3.03E-02 | 1.42 | 0.39 |
| 16575 HISTONE DEACETYLATION | -1.50 | 2.28E-02 | -0.53 | 0.50 |
| 10212 RESPONSE TO IONIZING RADIATION | -1.54 | 7.97E-03 | -1.50 | 0.03 |
| 51091 POSITIVE REGULATION OF SEQUENCE-SPECIFIC DNA BINDING TRANSCRIPTION FACTOR ACTIVITY | -1.68 | 3.19E-02 | 0.26 | 0.67 |
| 42393 HISTONE BINDING | -1.73 | 1.10E-02 | 1.09 | 0.36 |
| 12 SINGLE STRAND BREAK REPAIR | -1.83 | 6.86E-03 | -0.09 | 0.94 |
| 120 RNA POLYMERASE I TRANSCRIPTION FACTOR COMPLEX | -1.88 | 4.48E-05 | -0.53 | 0.49 |
| 51090 REGULATION OF SEQUENCE-SPECIFIC DNA BINDING TRANSCRIPTION FACTOR ACTIVITY | -1.93 | 2.32E-02 | -0.39 | 0.69 |
| 3684 DAMAGED DNA BINDING | -2.14 | 3.20E-02 | 0.14 | 0.87 |
| 16564 TRANSCRIPTION REPRESSOR ACTIVITY | -2.21 | 1.62E-02 | -1.25 | 0.28 |
| 122 NEGATIVE REGULATION OF TRANSCRIPTION FROM RNA POLYMERASE II PROMOTER | -2.47 | 3.97E-03 | 0.54 | 0.58 |
| 123 HISTONE ACETYLTRANSFERASE COMPLEX | -2.47 | 5.00E-02 | -0.12 | 0.89 |
| 4386 HELICASE ACTIVITY | -2.52 | 4.43E-04 | -0.72 | 0.43 |
| 16874 LIGASE ACTIVITY | -2.67 | 2.96E-03 | -1.52 | 0.09 |
| 4402 HISTONE ACETYLTRANSFERASE ACTIVITY | -2.78 | 1.41E-03 | -0.32 | 0.66 |
| 6310 DNA RECOMBINATION | -2.87 | 3.88E-03 | -1.29 | 0.08 |
| 6974 RESPONSE TO DNA DAMAGE STIMULUS | -3.19 | 1.60E-03 | 0.22 | 0.82 |
| 16571 HISTONE METHYLATION | -3.38 | 2.90E-04 | -1.31 | 0.23 |
| 16573 HISTONE ACETYLATION | -3.54 | 9.99E-04 | -0.50 | 0.53 |
| 6281 DNA REPAIR | -4.16 | 1.09E-05 | -0.68 | 0.49 |
| 6355 REGULATION OF TRANSCRIPTION, DNA-TEMPLATED | -5.46 | 3.27E-07 | -1.76 | 0.09 |
| 6350 TRANSCRIPTION | -5.77 | 9.27E-09 | -1.62 | 0.11 |

**Table S1, related to figure 7.** A list of Gene Ontology Terms that are significantly changed when comparing old $Csb^{m/m}$ saline treated mice vs old WT saline treated and old $Csb^{m/m}$ nicotinamide riboside treated mice vs old WT saline mice.

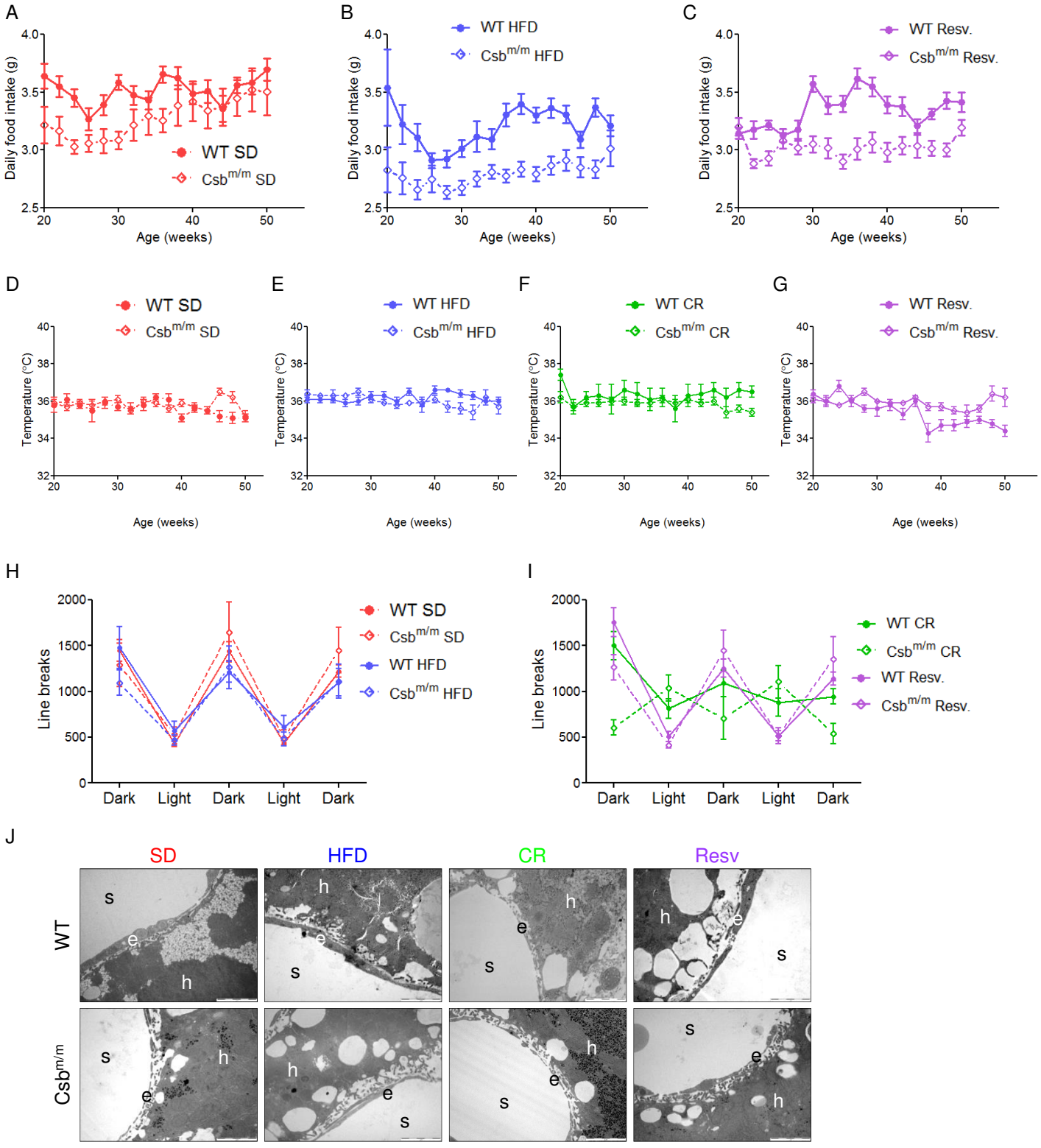
A
Daily food intake (g)
Age (weeks)
WT SD
Csb^m/m SD
B
WT HFD
Csb^m/m HFD
C
WT Resv.
Csb^m/m Resv.
D
Temperature (°C)
E
F
WT CR
Csb^m/m CR
G
H
Line breaks
Dark
Light
I
J
SD
HFD
CR
Resv
WT
Csb^m/m
s
e
h

Figure S1

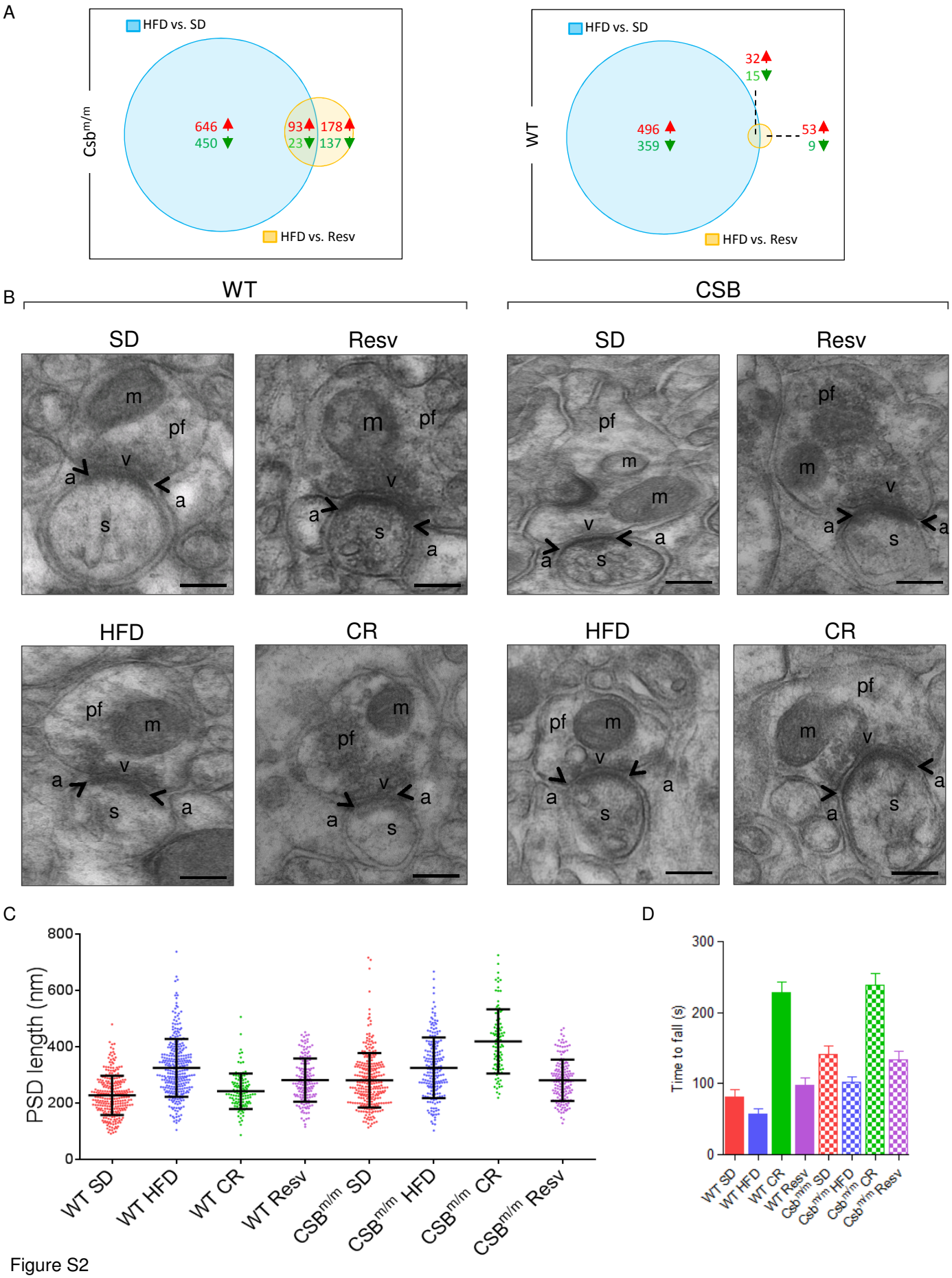
A
HFD vs. SD
Csb m/m
646
450
93
23
178
137
HFD vs. Resv
HFD vs. SD
WT
32
15
496
359
53
9
HFD vs. Resv
B
WT
CSB
SD
Resv
SD
Resv
HFD
CR
HFD
CR
m
pf
v
a
s
C
PSD length (nm)
800
600
400
200
0
WT SD
WT HFD
WT CR
WT Resv
CSB m/m SD
CSB m/m HFD
CSB m/m CR
CSB m/m Resv
D
Time to fall (s)
300
200
100
0
WT SD
WT HFD
WT CR
WT Resv
Csb m/m SD
Csb m/m HFD
Csb m/m CR
Csb m/m Resv

Figure S2

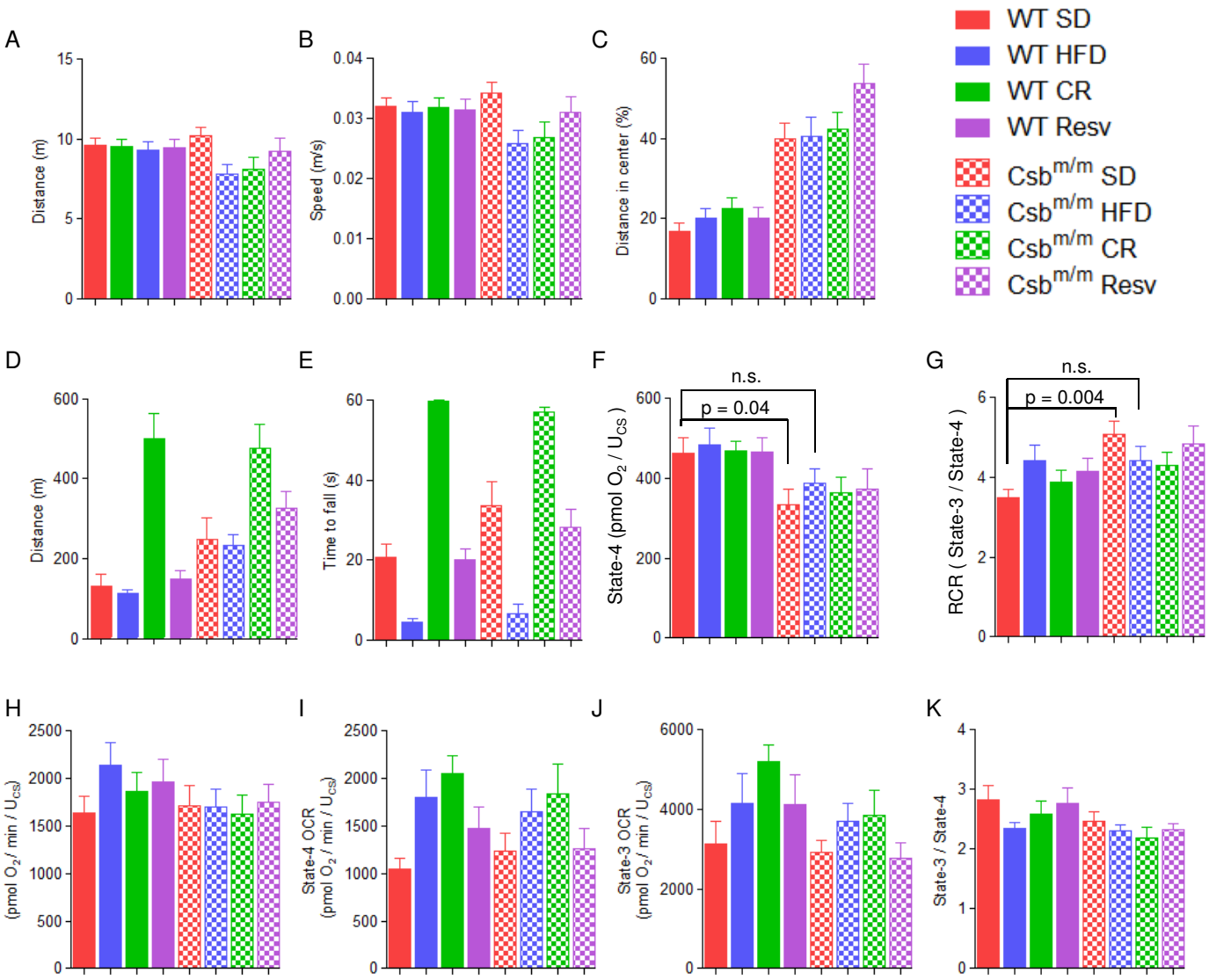
A
B
C
D
E
F
G
H
I
J
K
WT SD
WT HFD
WT CR
WT Resv
Csb m/m SD
Csb m/m HFD
Csb m/m CR
Csb m/m Resv
Distance (m)
Speed (m/s)
Distance in center (%)
Time to fall (s)
State-4 (pmol O2 / UCS )
RCR ( State-3 / State-4 )
State-3 OCR (pmol O2 / min / UCS)
State-4 OCR (pmol O2 / min / UCS)
State-3 / State-4
n.s.
p = 0.04
p = 0.004

Figure S3

A

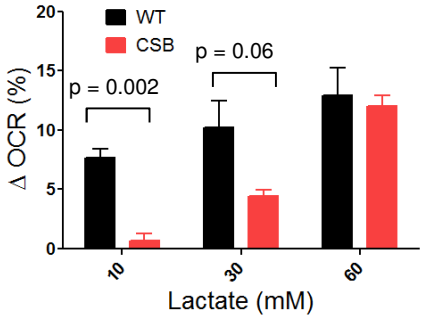


B

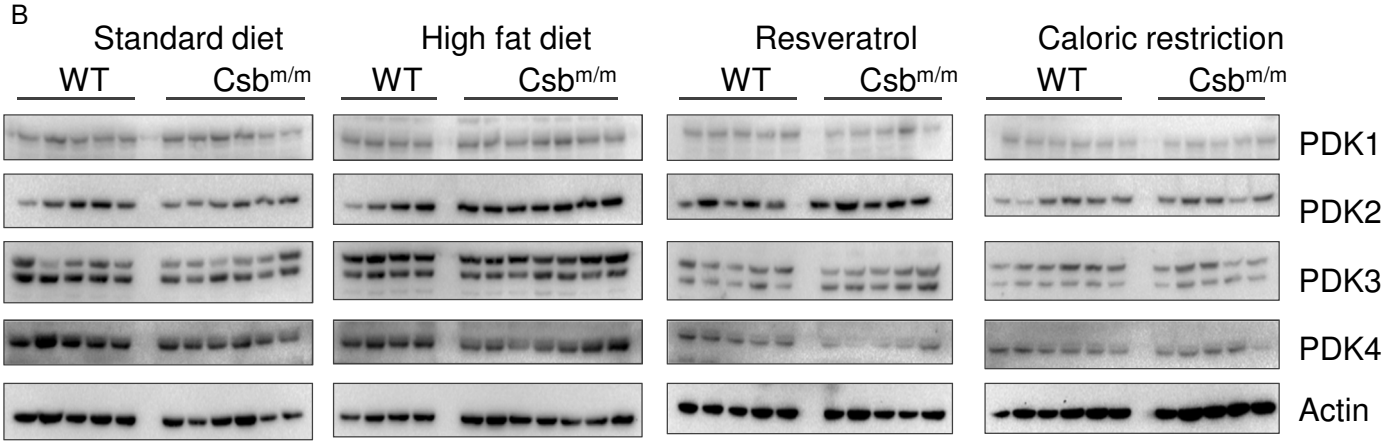


C

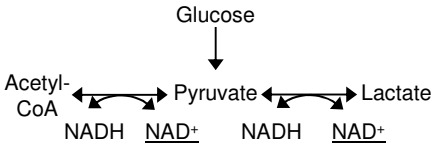


Figure S4

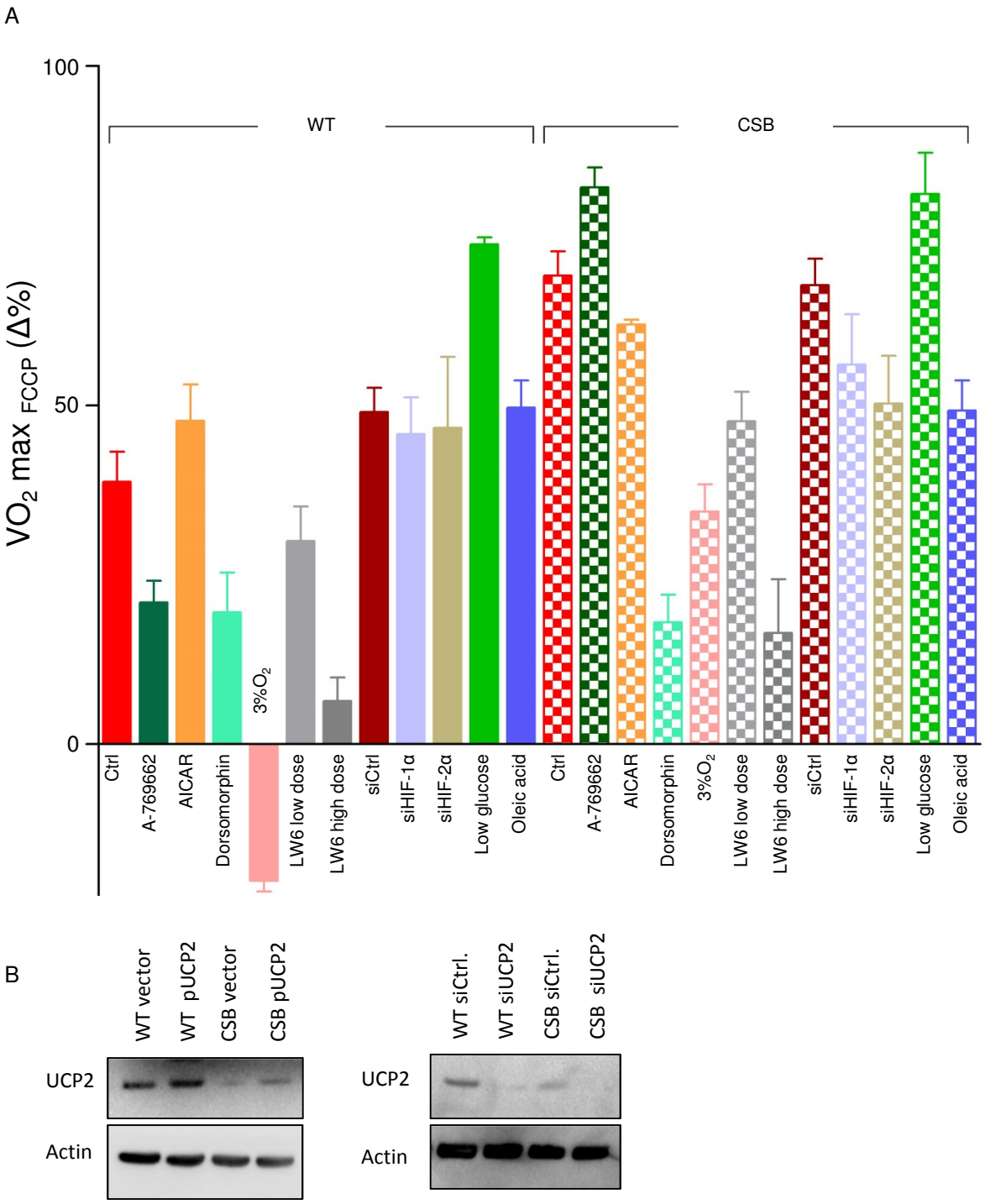
A
100
50
0
$VO_2$ max $_{FCCP}$ (Δ%)
WT
CSB
Ctrl
A-769662
AICAR
Dorsomorphin
3%$O_2$
LW6 low dose
LW6 high dose
siCtrl
siHIF-1α
siHIF-2α
Low glucose
Oleic acid
Ctrl
A-769662
AICAR
Dorsomorphin
3%$O_2$
LW6 low dose
LW6 high dose
siCtrl
siHIF-1α
siHIF-2α
Low glucose
Oleic acid
B
WT vector
WT pUCP2
CSB vector
CSB pUCP2
UCP2
Actin
WT siCtrl.
WT siUCP2
CSB siCtrl.
CSB siUCP2
UCP2
Actin

Figure S5

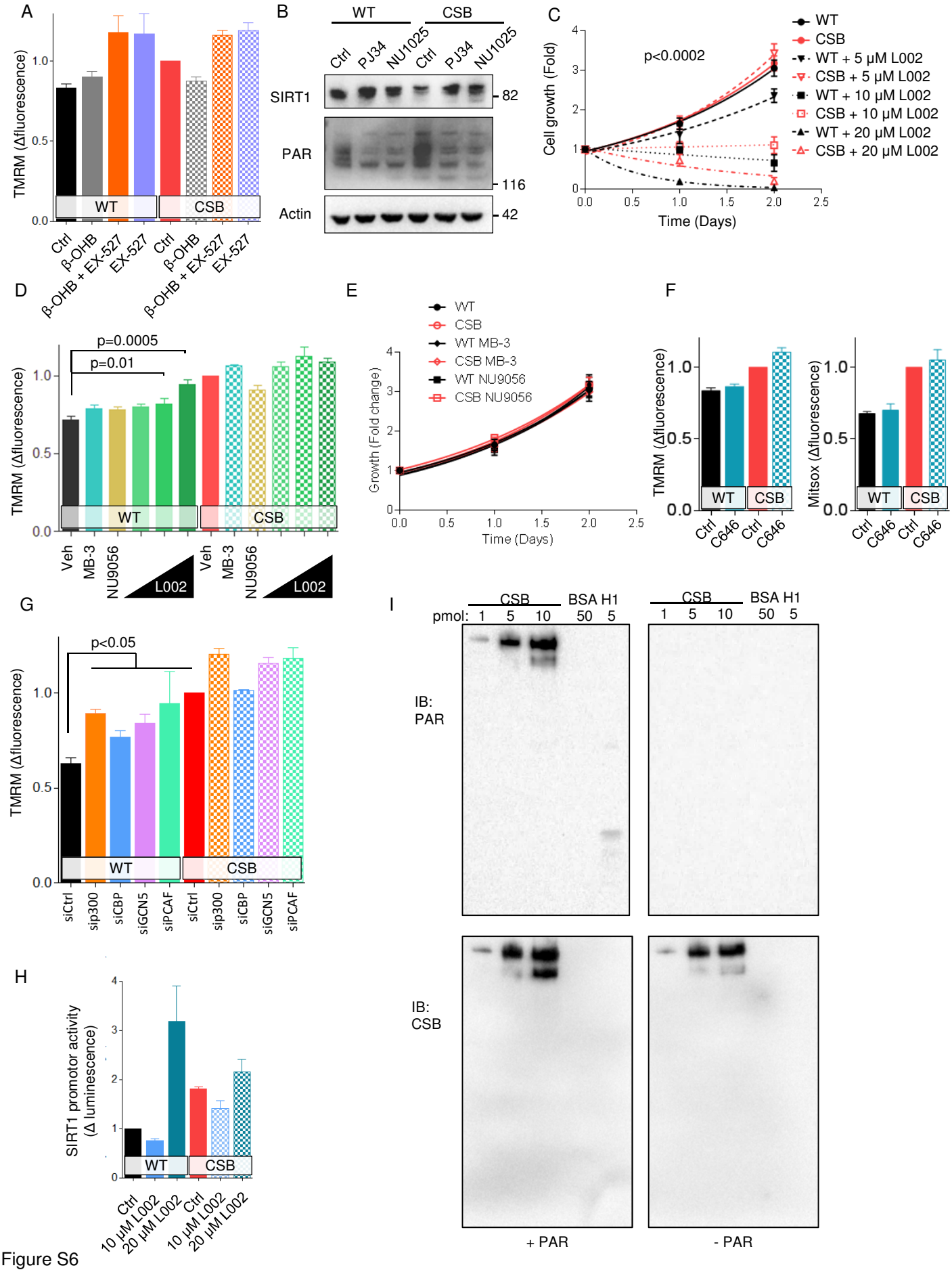
A
TMRM (Δfluorescence)
WT
CSB
Ctrl
β-OHB
β-OHB + EX-527
EX-527
B
WT
CSB
Ctrl
PJ34
NU1025
SIRT1
PAR
Actin
82
116
42
C
Cell growth (Fold)
p<0.0002
Time (Days)
WT
CSB
WT + 5 μM L002
CSB + 5 μM L002
WT + 10 μM L002
CSB + 10 μM L002
WT + 20 μM L002
CSB + 20 μM L002
D
TMRM (Δfluorescence)
p=0.0005
p=0.01
Veh
MB-3
NU9056
L002
E
Growth (Fold change)
Time (Days)
WT
CSB
WT MB-3
CSB MB-3
WT NU9056
CSB NU9056
F
TMRM (Δfluorescence)
Mitsox (Δfluorescence)
Ctrl
C646
G
TMRM (Δfluorescence)
p<0.05
siCtrl
sip300
siCBP
siGCN5
siPCAF
H
SIRT1 promotor activity
(Δ luminescence)
Ctrl
10 μM L002
20 μM L002
I
CSB
BSA H1
pmol: 1 5 10 50 5
IB:
PAR
IB:
CSB
+ PAR
- PAR

Figure S6